CHEMPHYSCHEM

DOI: 10.1002/cphc.200600675

Controlled Metalation of Self-Assembled Porphyrin Nanoarrays in Two Dimensions

Willi Auwärter,*[a] Alexander Weber-Bargioni,[a] Susan Brink,[b] Andreas Riemann,[a] Agustin Schiffrin,[a] Mario Ruben,[b] and Johannes V. Barth[a]

We report a bottom-up approach for the fabrication of metallo-porphyrin compounds and nanoarchitectures in two dimensions. Scanning tunneling microscopy and tunneling spectroscopy observations elucidate the interaction of highly regular porphyrin layers self-assembled on a Ag(111) surface with iron monomers supplied by an atomic beam. The Fe is shown to be incorporated selectively in the porphyrin macrocycle whereby the template structure is strictly preserved. The immobilization of the molecular reactants allows the identification of single metalation events in a novel reaction scheme. Because the template layers provide extended arrays of reaction sites, superlattices of coordinatively unsaturated and magnetically active metal centers are obtained. This approach offers novel pathways to realize metallo-porphyrin compounds, low-dimensional metal-organic architectures and patterned surfaces which cannot be achieved by conventional means.

Introduction

The control of matter at the molecular level is of paramount importance for the development of novel materials and functional device architectures.[1,2] Well-defined surfaces are particularly useful in this respect, because they represent versatile platforms to engineer molecular architectures with exquisite feature control, which can be examined and manipulated at the nanoscale by scanning tunneling microscopy (STM). Thus a variety of molecular building blocks have been successfully employed to assemble functional layers and nanostructures on surfaces, notably exploiting complex molecular species. Here we focus on the synthesis and organization of novel porphyrin nanoarchitectures in two dimensions. Porphyrins exhibit an intriguing variety of functional properties, which are exploited in both biological and artificial systems.[3] Particularly interesting are the Fe-porphyrins, which play (as hemes) a central role in life processes encompassing transport of respiratory gases and catalytic functions.[4,5] Accordingly, these versatile molecules are promising building blocks to assemble functional layers and nanostructures on surfaces, specifically opening up new opportunities to build sensors, and nanoscale optical and magnetic materials.[6,7]

The functionality and self-assembly of porphyrins is based on three main features: 1) the porphyrin core macrocycle can host a wide range of metals, which present active sites to reversibly form porphyrin-ligand complexes.[8,9] 2) Porphyrins with a wide variety of *meso*-substituents can be synthesized. They determine the molecules' functional properties and render building blocks for metal-organic networks in solid state chemistry[10] and 2-D molecular engineering.[2,11–16] 3) The flexibility of the porphyrin core and the rotational degrees of freedom of the *meso*-groups allow for a conformational adaptation of the molecule to its local environment[12,17] and their considerate manipulation.[18–20] Here we present a molecular-level investigation on a novel scheme for the fabrication of metallo-tetraarylporphyrins in two dimensions (2D) employing STM and scanning tunneling spectroscopy (STS). The starting point are terapyridylporphyrin (TPyP) layers self-assembled on the Ag(111) surface, which are shown to be highly reactive towards Fe centers provided by an atomic beam. The resulting compounds exhibit structural and electronic characteristics strongly indicating complexation at very unusual reaction conditions. This interpretation is corroborated by a careful comparison with the structural and electronic properties of the related species Fe^{II}-tetraphenylporphyrin (Fe-TPP) deposited on the same substrate.

Results and Discussion

The individual steps in the formation of metallo-porphyrin compounds and highly organized nanoarrays in two dimensions are demonstrated using well-defined tetrapyridylporphyrin (H_2-TPyP) template layers. Figure 1a shows a structural model of the free base H_2-TPyP molecule, our starting material, which consists of the central porphyrin macrocycle and four

[a] *Dr. W. Auwärter, A. Weber-Bargioni, Dr. A. Riemann, A. Schiffrin, Prof. Dr. J. V. Barth*
Departments of Chemistry and Physics & Astronomy
University of British Columbia
Vancouver, B.C. V6T 1Z4 (Canada)
Fax: (+1) 604 822 4750
E-mail: auwarter@phas.ubc.ca

[b] *Dr. S. Brink, Dr. M. Ruben*
Institut für Nanotechnologie, Forschungszentrum Karlsruhe
76021 Karlsruhe (Germany)

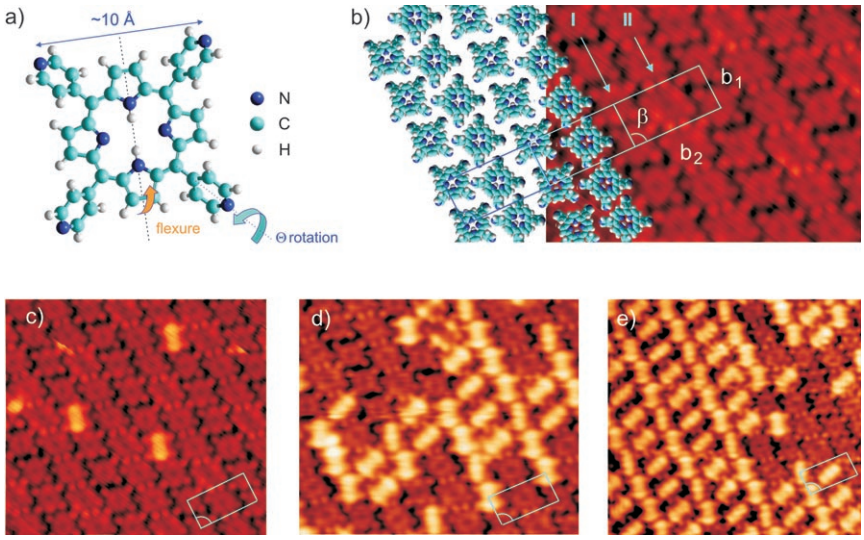

Figure 1. a) Structure model of H_2-TPyP (top view). The dashed line indicates the molecular symmetry axis as referred to in the text. b) Self-assembled H_2-TPyP layer on Ag(111). The domain comprises two distinguishable types of rows (I, II) with a different azimuthal orientation of the molecules, which are marked by arrows. c)-e) Reaction of a H_2-TPyP precursor layer with Fe. The appearance of individual molecules is drastically altered. By increasing the Fe dose, their number can be tuned from zero to full saturation. As indicated by the unit cell, the molecular packing remains unaffected by the reaction. (b, c: $V_{Sample} = -1.2$ V, $I = 0.7$ nA, and d, e: $V_{Sample} = -0.3$ V, $I = 0.85$ nA).

terminal pyridyl rings. Upon adsorption on Ag(111) the porphyrin board is oriented parallel to the surface, while the pyridyl rings alternately rotate out of the porphyrin plane by a dihedral angle of about 60°, resulting in a rectangular envelope of the molecule in the STM topography[21] (Figure 1 b). Moreover, the surface mobility and lateral interactions enable the self-assembly of well-ordered two-dimensional molecular domains extending over hundreds of nanometers even at room temperature. The high-resolution STM image depicted in Figure 1 b reveals the molecular packing and intramolecular features. The H_2-TPyP molecules order in a staggered arrangement. Besides the porphyrin core with a depression in the center, four protrusions corresponding to the pyridyl rings are clearly discernible. Two different molecular orientations (labeled I and II, respectively) are observed in the imaged domain. This packing scheme can be described by a nearly rectangular unit cell with a molecule in every corner and a central molecule in a different azimuthal orientation.[21] The H_2-TPyP models in Figure 1 b including the unit cell ($b_1 = 13.9$ Å, $b_2 = 27.4$ Å) highlight the structure and facilitate the identification of the molecular moieties.

In the next step, we examine the reactivity of the well defined H_2-TPyP precursor layer toward Fe atoms provided by an atomic beam (cf. Figure 1 c–e). Upon exposure to minute amounts of Fe at 320 K the appearance of isolated molecules changes drastically. STM images recorded at negative sample voltages show that a unique new species evolves, which is imaged brighter exhibiting an increased apparent height of ≈0.7 Å compared to the H_2-TPyP precursor layer. Instead of the depression in the center, this species exhibits a central rodlike protrusion (≈12 Å long) which is always oriented along the molecular symmetry axis (here defined parallel to the short side of the rectangular envelope) and comprises two or three corrugation maxima. The number of modified molecules directly correlates with the Fe dose, as demonstrated by the image sequence in Figure 1. Our data clearly reveal a preserved 2D TPyP layer structure, where exclusively the central porphyrin moieties undergo drastic changes. We observe a spatially inhomogeneous distribution of Fe-TPyP for intermediate Fe doses, reflecting appreciable Fe mass transport on the H_2-TPyP layer, cooperative effects and an activation barrier relevant for this reaction. From now on we tentatively refer to the modified molecular species as Fe-TPyP.

Higher Fe doses allow the formation of regular Fe-TPyP arrays, where the alternating orientation of the Fe-induced features, nicely reflects the orientation of the H_2-TPyP template layer (Figure 2). The apparent height of the Fe-TPyP molecules as well as the corrugation within the layer depends on the sample bias voltage. Under typical imaging conditions ($V_{Sample} = -1$ V) we measure an apparent height of 1.9 Å and a corrugation of 0.7 Å, respectively. Figure 2 b shows height profiles along the molecular axis of two Fe-TPyP molecules in the same row. As mentioned before, between two and three protrusions are observed. This variation in the topographic appearance, observed in both types of molecular rows, is induced by inequivalent adsorption sites of the molecules on the underlying substrate lattice: The TPyP overlayer is not commensurate with the Ag(111) surface, resulting in a Moiré pattern with subtle long-range height modulations.[21]

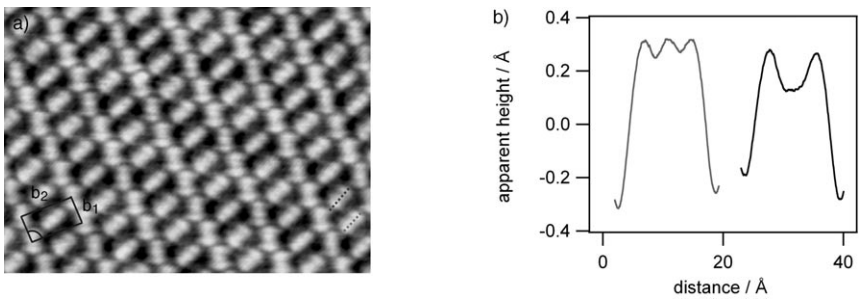

Figure 2. a) STM image showing the regular ordering of a fully developed Fe-TPyP array, representing the completion of the image series in Figure 1 c–e ($V_{Sample} = -0.4$ V, $I = 0.65$ nA). b) Two height profiles representing the dashed lines in (a).

In order to investigate the nature of the Fe-TPyP molecules and to rationalize the origin of their drastically modified appearance in the STM topography we performed comparative experiments with Fe^{II}-tetraphenylporphyrin (Fe-TPP) layers self-assembled on Ag(111). TPP consists of a central porphyrin macrocycle and four terminal phenyl rings, and thus closely resembles TPyP. Each Fe-TPP comprises a Fe^{II} center in the porphyrin plane (inset Figure 3).[22] The self-assembly of this species on Ag(111) can be conducted with similar procedures as those employed for H_2-TPyP. An example for a highly regular Fe-TPP layer on Ag(111) is reproduced in the STM image in Figure 3. These data expose a striking similarity of the intramolecular features dominated by the porphyrin cores comprising the iron with the Fe-TPyP species shown in Figure 2. Again, the topographic appearance is dominated by two or three protrusions along the molecular axis. The height profiles in Figure 3b accentuate this close resemblance.

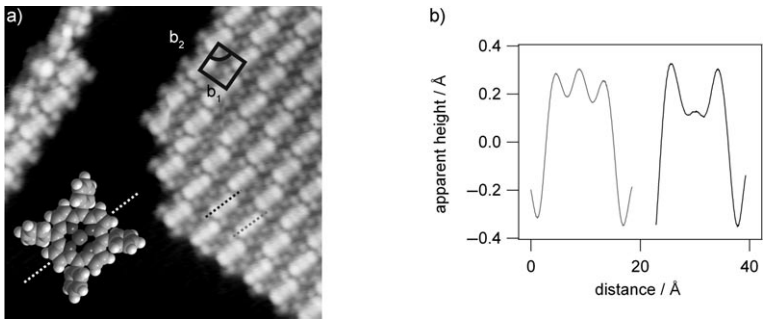

Figure 3. a) STM image of a Fe-TPP island exhibiting a molecular packing scheme described by a square unit cell with side lengths $b_1 = b_2 = 14.3 \pm 0.1$ Å ($V_{Sample} = -0.8$ V, $I = 0.65$ nA). Inset: model of a Fe-TPP molecule placed in the same azimuthal orientation as the Fe-TPP's in the STM image. b) Two height profiles along the molecular axis of the Fe-TPP molecules highlighted by the dashed line in (a). Note the close resemblance to the topography of Fe-TPyP shown in Figure 2b.

The data in Figure 3a reveal that regular Fe-TPP layers on Ag(111) exhibit a packing scheme with a correlated single azimuthal orientation of the molecules with respect to substrate high-symmetry directions. This distinction to the TPyP case arises from different lateral interactions due to a changed reactivity of the phenyl endgroups in comparison to the pyridyl substituents. The square unit cell (side length $b_1 = b_2 = 14.3 \pm 0.2$ Å) we observe, agrees with observations of related metal-TPP molecules on close-packed noble metal surfaces.[23,24]

The isostructural intramolecular features in the Fe-TPyP- and Fe-TPP-layers are a strong indication that in both cases genuine Fe^{II}-porphyrin species are present. The appearance of the Fe-porphyrins revealing an apparent symmetry break characterized by the pronounced protrusions along the molecular axis, is associated with a nonplanar geometry of the porphyrin macrocycle. While undistorted porphyrin species feature a four-fold symmetric core appearance (Figure 1), nonplanar deformations result in pronounced protrusions establishing a two-fold symmetry of the porphyrin macrocycle.[12,19,20] Fe-tetraarylporphyrin species with a saddle shape are well-known and can serve as a tentative explanation of the observed features.[25,26] In this nonplanar deformation one opposing pair of pyrrole rings tilts up, while the other pair tilts down. Judging from the molecular dimensions the two outer protrusions originate from the upwards bent pyrrole pair, while the central protrusion relates to the Fe ion. The fact that the terminal groups are alternately rotated out of the porphyrin plane allows only one pyrrole pair to tilt up, while the other pair is hindered by steric repulsion between hydrogen atoms of the ring and the terminal groups. Thus, we observe the protrusion exclusively along a specific symmetry axis in the 2D porphyrin layers.

In most cases described so far the nonplanar molecules are Fe^{III} species where the axial ligands induce molecular flexure.[27,28] The coupling of the present Fe-porphyrins to the Ag(111) substrate seems to induce similar structural distortions. We expect that the molecular conformation can be influenced by the choice of the employed substrate and by reacting the metallo-porphyrin layers with appropriate axial ligands. Because the electronic and magnetic, but also catalytic, properties of the complexes depend sensitively on these parameters, Fe-porphyrin layers represent an interesting playground to investigate the magnetic and biological properties of metalated porphyrin compounds on surfaces.

The conclusions drawn from the structural analysis are substantiated by STS observations which elucidate the electronic properties of the different (metallo-)porphyrin species. The data in Figure 4d reveal that the steplike increase in the STS spectra resulting from the onset of the Ag(111) surface state at an energy of -65 meV[29,30] disappears upon the formation of the pure H_2-TPyP layers. The latter exhibit rather a pronounced feature at $+740$ meV associated with the TPyP's two lowest unoccupied molecular orbitals (LUMOs), which are energetically very close in the isolated porphyrin molecule.[31,32] By contrast, the Fe-TPyP and Fe-TPP LUMO levels shown in Figure 4e are shifted towards higher energies and are found at 990 and 1020 meV, respectively. The plotted spectra represent a sum over several identical molecules as well as a spacial average over different spots on a molecule. The upward shift is in agreement with spectroscopic observations[33] and theoretical calculations.[32] It arises from the interactions between the LUMOs and the filled d_π metal orbitals and has a direct impact on the topographic imaging of H_2-TPyP and Fe-TPyP in constant current STM images (Figure 4 a–c). At negative sample voltages the Fe-TPyP molecules appear brighter than the H_2-TPyP species (Figure 1 c-e and Figure 4a), while tuning the sample voltage to a positive value between the H_2-TPyP and Fe-TPyP LUMO energies results in a contrast inversion (Figure 4b), as the Fe-TPyP LUMO does not mediate electron tunneling. At voltages well above the upshifted Fe-TPyP LUMO levels (Figure 4c) the two porphyrin species are essentially indistinguishable, in full agreement with the spectroscopic data.

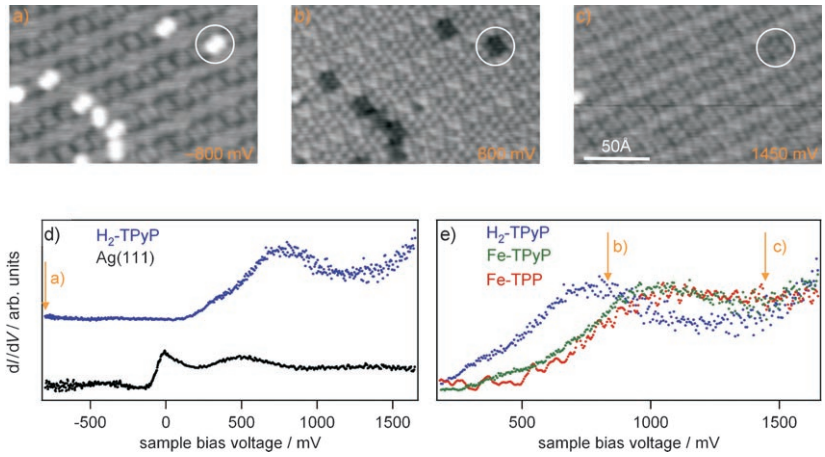

Figure 4. a)–c) Chemical sensitivity through bias-dependent imaging of H_2-TPyP and Fe-TPyP. The relative apparent height and appearance of H_2-TPyP and Fe-TPyP is strongly bias voltage dependent due to metalation induced modifications of the molecular electronic structure, as outlined in (d) and (e). The circle highlights the position of one specific Fe-TPyP molecule (see text). All three images are taken at a set point current of 0.71 nA. d) Tunneling spectra taken on bare Ag(111) and on H_2-TPyP. The two spectra are shifted by a vertical offset for clarity. e) Comparison of the H_2-TPyP with the Fe-TPyP and Fe-TPP tunneling spectra. The yellow arrows indicate the bias voltages used to acquire the images a), b) and c), respectively.

The voltage-dependent topography of Fe-TPP is very similar to that of Fe-TPyP.[34] The almost identical LUMO shift for both Fe-TPyP and Fe-TPP (Figure 4e) is ascribed to the fact that these molecular orbitals have major electron densities only at the porphyrin core, hence their energetics are hardly affected by the different *meso* substituents.[13,32]

Thus both the structural analysis and the electronic structure characteristics of the three porphyrin species evidence a metalation reaction upon exposing adsorbed H_2-TPyP to Fe atoms. This implies that the metalloporphyrin formation readily occurs in situ on the surface. The corresponding reaction is schematically illustrated in Figure 5. It is formally described by Equation (1):

$$H_2\text{-TPyP} + Fe \Rightarrow Fe\text{-TPyP} + H_2 \Uparrow \quad (1)$$

In this process, schematically, the two pyrrolic protons will be reduced to molecular hydrogen (H_2) by the simultaneous oxidation of the incoming Fe^0 center to Fe^{II}. Due to the affinity of Fe for axial ligands,[32] intermediate product H atoms might be transiently attached to the Fe centers before recombining to H_2 which is thermally desorbed. This drives the redox reaction to completion and establishes local electroneutrality between the metallic Fe^{II} centre and the organic tetrapyridylporphyrinato dianion. Thus, we expect the Fe ion to be in the Fe^{II} oxidation state, analogous to the Fe-TPP molecules used as a reference in these experiments. The mechanism described here provides a simple and general picture which does not take into account explicitly the influence of the substrate. The latter acts as an anchoring surface with a periodic potential which influences the relative geometry of the reactants, as well as an electron source which can screen the electrical charges held by the adsorbates. The indirect participation of the substrate in the chemical reaction is therefore an important factor, and was similarly encountered in the complexation of metal centers by carboxylate species on surfaces.[35–37]

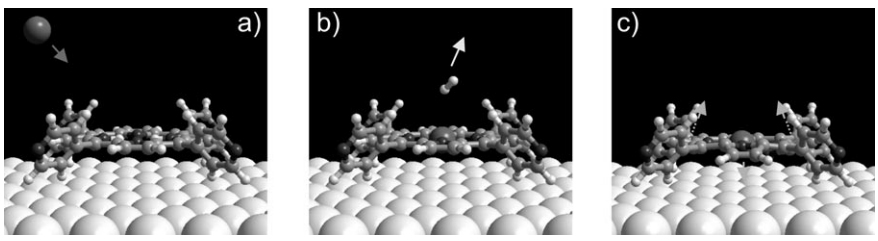

Figure 5. Representation of the three main processes during the formation of a metallo-porphyrin on a surface. a) Pure H_2-TPyP layer is exposed to Fe atoms from an atomic beam. b) Pyrrolic protons are reduced to molecular hydrogen which desorbs while the Fe is oxidized and incorporated into the dianionic porphyrinato core. c) Induction of a nonplanar deformation of the porphyrin macrocycle on Ag(111). The saddle shaped geometry is indicated by the arrows and explains the protrusions along one molecular axis observed in the STM data.

Conclusions

In conclusion we demonstrated the formation of a Fe-tetrapyridylporphyrin on a Ag(111) surface based on a novel reaction scheme. This new approach opens up some appealing opportunities, especially as it seems easily applicable to a large variety of porphyrin species on surfaces which can be metalated by Fe and presumably other metal centers. Specifically, it allows the formation of low-dimensional metallo-porphyrin architectures by using preorganized porphyrin arrangements which are subsequently functionalized by metal centers. Moreover novel porphyrin compounds can be created, because procedures can be implemented where the addition of the metal center appears as a final step.

In short, the methodology presented here is expected to provide a basis for the synthesis of high-purity metalloporphyrin nanostructures on surfaces, which could not be obtained by conventional methods as organic molecular beam epitaxy or deposition in solution, due to a limited thermal stability and/or high reactivity of the metalloporphyrins. Especially, the availability of the axial position of the metal centers for further reaction with biological relevant ligands (O_2, CO, etc.) opens the possibility to carry out biological relevant reaction schemes.

Note added: After the completion of this manuscript we noticed that a preliminary presenta-

tion of our approach[38] inspired a study using a space averaging method (XPS) that confirms the finding of porphyrin metalation on surfaces.[39]

Experimental Section

All experiments were performed with a custom-designed ultrahigh vacuum (UHV) apparatus comprising a commercial low-temperature scanning tunneling microscope (http://www.lt-stm.com/) based on the design described in ref. [40]. The STM was operated typically at 15 K to obtain high-resolution topographic and spectroscopic data. The STM tip is made out of an etched W wire (Ø 0.3 mm) and was prepared by Ar-bombardment in UHV. Topographic data were acquired in the constant current mode, with typical tunneling resistances in the range of 10–10^4 MΩ. In the Figure captions *V* refers to the bias voltage applied to the sample. Tunneling spectroscopy data were recorded with a lock-in technique (typical modulation amplitude and frequency 20 mV and 1 kHz, respectively).

The system base pressure was below 2×10^{-10} mbar. The Ag(111) surface was prepared by repeated cycles of argon sputtering (800 eV, 8 μA/cm^2) followed by annealing at 750 K.

TPyP (Scheme 1) was obtained from Frontier Scientific (97 + % purity). The FeTPP molecules were synthesized following an adapted procedure described in literature using hydrazine as the reducing medium.[22] Care was taken not to expose the FeTPP to air in view of their well-known reactivity towards oxygen.[41] Accordingly the molecules were always transferred to UHV under inert gas atmosphere. The porphyrins were first outgassed in vacuum for several hours and then evaporated from an organic molecular beam epitaxy cell at 525 K onto the substrate kept at 330 K. This provided a deposition rate of about 0.05 monolayers (ML) per minute. Fe atoms were evaporated from a home-made water-cooled cell by resistively heating a W filament surrounded by an Fe wire of high purity (99.998%). During Fe deposition the substrate was held at 320 K.

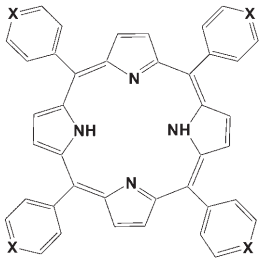

Scheme 1. Structure of the free base TPyP and TPP molecules.

Acknowledgements

Work supported by the Swiss National Science Foundation through a postdoctoral scholarship for W. A., and by DAAD through a PhD stipendium for A.W., CFI and BCKDF, NSERC, ESF-SONS-FunSMARTs. We thank A.P. Seitsonen for helpful discussions.

Keywords: iron · metalation · porphyrin · scanning probe microscopy · self-assembly

[1] B. D. Gates, Q. Xu, M. Stewart, D. Ryan, C. G. Willson, G. M. Whitesides, *Chem. Rev.* **2005**, *105*, 1171.
[2] J. V. Barth, G. Costantini, K. Kern, *Nature* **2005**, *437*, 671.
[3] D. Dolphin, *The Porphyrins*, Academic, New York, **1978**.
[4] L. R. Milgrom, *The Colours of Life: An Introduction to the Chemistry of Porphyrins and Related Compounds*, Oxford University Press, **1997**.
[5] J. T. Groves, *PNAS* **2003**, *100*, 3569.
[6] K. M. Kadish, K. M. Schmith, R. Guilard, *The Porphyrin Handbook, Vol. 6*, Academic Press, San Diego, **2000**.
[7] J. A. A. W. Elemans, R. v. Hameren, R. J. M. Nolte, A. E. Rowan, *Adv. Mater.* **2006**, *18*, 1251.
[8] F. J. Williams, O. P. H. Vaughan, K. J. Knox, N. Bambos, R. M. Lambert, *Chem. Commun.* **2004**, 1688.
[9] O. Shoji, H. Tanaka, T. Kawai, Y. Kobuke, *J. Am. Chem. Soc.* **2005**, *127*, 8598.
[10] M. E. Kosal, K. S. Suslick, *J. Solid State Chem.* **2000**, *152*, 87.
[11] M. Kunitake, N. Batina, K. Itaya, *Langmuir* **1995**, *11*, 2337.
[12] T. Yokoyama, S. Yokoyama, T. Kamikado, S. Mashiko, *Journal of Chemical Physics* **2001**, *115*, 3814.
[13] L. Scudiero, D. E. Barlow, K. W. Hipps, *J. Phys. Chem. B* **2002**, *106*, 996.
[14] D. Bonifazi, H. Spillmann, A. Kiebele, M. d. Wild, P. Seiler, F. Cheng, H.-J. Güntherodt, T. Jung, F. Diederich, *Angew. Chem.* **2004**, *116*, 4863; *Angew. Chem. Int. Ed.* **2004**, *43*, 4759.
[15] M. Abel, V. Oison, M. Koudia, C. Maurel, C. Katan, L. Porte, *ChemPhysChem* **2006**, *7*, 82.
[16] K. W. Hipps, L. Scudiero, D. E. Barlow, M. P. Cooke, *J. Am. Chem. Soc.* **2002**, *124*, 2126.
[17] T. A. Jung, R. R. Schlittler, J. K. Gimewski, *Nature* **1997**, *386*, 696.
[18] C. Loppacher, M. Guggisberg, O. Pfeiffer, E. Meyer, M. Bammerlin, R. Luthi, R. Schlittler, J. K. Gimzewski, H. Tang, C. Joachim, *Phys. Rev. Lett.* **2003**, *90*, 066107.
[19] X. H. Qiu, G. V. Nazin, W. Ho, *Phys. Rev. Lett.* **2004**, *93*, 196806.
[20] V. Iancu, A. Deshpande, S.-W. Hla, *Nano Lett.* **2006**, *6*, 820.
[21] W. Auwärter, A. Weber-Bargioni, A. Riemann, A. Schiffrin, O. Groening, R. Fasel, J. V. Barth, *J. Chem. Phys.* **2006**, *124*, 194708.
[22] J. P. Collman, J. L. Hoard, N. Kim, G. Lang, C. A. Reed, *J. Am. Chem. Soc.* **1975**, *97*, 2676.
[23] L. Scudiero, D. E. Barlow, K. W. Hipps, *J. Phys. Chem. B* **2000**, *104*, 11899.
[24] K. Suto, S. Yoshimoto, K. Itaya, *J. Am. Chem. Soc.* **2003**, *125*, 14976.
[25] J. A. Shelnutt, X.-Z. Song, J. G. Ma, S.-L. Jia, W. Jentzen, C. J. Medforth, *Chemical Society Reviews* **1998**, *27*, 31.
[26] H. M. Marques, K. L. Brown, *Coord. Chem. Rev.* **2002**, *225*, 123.
[27] R.-J. Cheng, P.-Y. Chen, P.-R. Gau, C.-C. Chen, S.-M. Peng, *J. Am. Chem. Soc.* **1997**, *119*, 2563.
[28] T. Ikeue, Y. Ohgo, T. Yamaguchi, M. Takahashi, M. Takeda, M. Nakamura, *Angew. Chem.* **2001**, *113*, 2687; *Angew. Chem. Int. Ed.* **2001**, *40*, 2617.
[29] J. Li, W.-D. Schneider, R. Berndt, O. R. Bryant, S. Crampin, *Phys. Rev. Lett.* **1998**, *81*, 4464.
[30] F. Reinert, G. Nicolay, S. Schmidt, D. Ehm, S. Hüfner, *Phys. Rev. B* **2001**, *63*, 115415.
[31] D. Lamoen, M. Parrinello, *Chem. Phys. Lett.* **1996**, *248*, 309.
[32] M.-S. Liao, S. Scheiner, *J. Chem. Phys.* **2002**, *117*, 205.
[33] K. S. Suslick, R. A. Watson, *New. J. Chem.* **1992**, *16*, 633.
[34] A. Weber-Bargioni, W. Auwärter, A. Schiffrin, Y. Pennec, J. V. Barth, **2006** unpublished results.
[35] N. Lin, A. Dmitriev, J. Weckesser, J. V. Barth, K. Kern, *Angew. Chem.* **2002**, *114*, 4973; *Angew. Chem. Int. Ed.* **2002**, *41*, 4779.
[36] S. Clair, S. Pons, S. Fabris, S. Baroni, H. Brune, K. Kern, J. V. Barth, *J. Phys. Chem. B* **2006**, *110*, 5627.
[37] A. P. Seitsonen, M. Lingenfelder, H. Spillmann, A. Dmitriev, S. Stepanow, N. Lin, K. Kern, J. V. Barth, *J. Am. Chem. Soc.* **2006**, *126*, 5634.
[38] W. Auwärter, A. Weber-Bargioni, A. Riemann, A. Schiffrin, J. V. Barth, in *ECOSS 23*, Berlin, **2005**, p. 36.
[39] J. M. Gottfried, K. Flechtner, A. Kretschmann, T. Lukasczyk, H.-P. Steinrück, *J. Am. Chem. Soc.* **2006**, *128*, 5644.
[40] G. Meyer, *Rev. Sci. Instrum.* **1996**, *67*, 2960.
[41] C. Hu, A. Roth, M. K. Ellison, J. An, C. M. Ellis, C. E. Schulz, W. R. Scheidt, *J. Am. Chem. Soc.* **2005**, *127*, 5675.

Received: October 28, 2006
Published online on December 14, 2006

